Commuting quantum transfer-matrix approach to intrinsic fermion system: Correlation length of a spinless fermion model

Kazumitsu Sakai, Masahiro Shiroishi, and Junji Suzuki*
Institute of Physics, University of Tokyo, Komaba 3-8-1, Meguro-ku, Tokyo 153-8902, Japan

Yukiko Umeno
Department of Physics, University of Tokyo, Hongo 7-3-1, Bunkyo-ku, Tokyo 113-0033, Japan
(Received 23 February 1999)

The quantum transfer-matrix approach to integrable lattice fermion systems is presented. As a simple case we treat the spinless fermion model with repulsive interaction in critical regime. We derive a set of nonlinear integral equations which characterize the free energy and the correlation length of $\langle c_j^\dagger c_i \rangle$ for an arbitrary particle density at any finite temperatures. The correlation length is determined by solving the integral equations numerically. Especially in the low-temperature limit this result agrees with the prediction from conformal field theory with high accuracy. [S0163-1829(99)13827-X]

I. INTRODUCTION

Exact evaluations of physical quantities at finite temperatures pose serious difficulties even for integrable models. One has to go much beyond mere diagonalization of a Hamiltonian; summation over the eigenspectra must be performed.

The string hypothesis[1–4] brought the first breakthrough and success. It yields a systematic way to evaluate several bulk quantities including specific heats, susceptibilities, and so on.

More recently, the quantum transfer-matrix (QTM) method has been proposed to overcome some difficulties, to which the standard approach is not applicable.[5–28] One reduces the original problem to finding the largest eigenvalue of the QTM which acts on a fictitious system of size N (referred to as the Trotter number), which should be sent $N \to \infty$ (Trotter limit). As this procedure is sometimes difficult, we integrate its procedure with another ingredient, the integrable structure of the underlying model. This allows for the introduction of commuting QTM's which are labeled by the complex parameter x.[14] A set of auxiliary functions, including the QTM itself, satisfy certain functional relations. We shall choose these functions such that they have an analytical property called ANZC (analytic, nonzero, and constant asymptotics; see Sec. III) in a certain strip on the complex x plane. This admits the transformation of the functional relations into a closed set of integral equations. For all cases known up to now, the Trotter limit $N \to \infty$ can be taken analytically in the integral equations. We thus have seen a remarkable reduction from the problem of combinatorics (summation over the eigenspectra) to the study of analytic structures of suitably chosen auxiliary functions.

This scenario has been applied to many models of physical interest.[14–27] In particular the correlation lengths, calculation of which has been one of the major difficulties in the string hypothesis, are explicitly evaluated in the spin models. For an example of the success achieved, we refer to a recent analysis on the quantum-classical crossover phenomena in the massless XXZ model in the "attractive" regime.[23,24]

We extend these studies to lattice fermion systems. Our formulation is fully general for one-dimensional (1D) fermion systems which are integrable in the sense of the Yang-Baxter (YB) equation. As a concrete example, we take the spinless fermion model with repulsive interactions in the gapless regime. This simple example already manifests some fundamental differences from the spin models, and yields a sound basis for future studies on more realistic fermion systems such as the Hubbard model.

As in Refs. 17–20, one may first perform Jordan-Wigner (JW) transformations to the fermion models, and further convert the resultant quantum spin models into 2D classical vertex models. These procedures have been successful in studies of the bulk quantities. In evaluating correlation lengths, however, this is no longer true. As an example, which will be discussed in the main body of this paper, let us take a fermion one-particle Green's function $\langle c_j^\dagger c_i \rangle$ and its correspondent $\langle \sigma_j^+ \sigma_i^- \rangle$ in the spin model. Obviously they are related, but quite different by nonlocal terms due to the JW transformation. At zero temperature $(T=0)$, using conformal mapping, one evaluates the scaling dimensions from finite size corrections to the energy spectra. As the Hamiltonians are equivalent through the JW transformations, it is normally difficult to discriminate between the energy spectra of the fermions and those of the spins. The difference lies only in the boundary conditions. Nevertheless, even after JW transformation one can explicitly calculate the correct scaling dimensions only by incorporating the proper fermion statistics at the very last stage (see Appendix B). At finite temperature $(T>0)$, the QTM approach gives the correlation function in the spectral decomposition form as $\Sigma_k |A_k|^2 (\Lambda_k/\Lambda_1)^{j-i-1}$. Here Λ_k denotes the kth largest eigenvalue of the QTM, and A_k is a certain matrix element. Once the JW transformation is performed, it is difficult to trace the difference in the statistics in this framework. Then one hardly recognizes the difference in the eigenvalues of the QTM between the spin models and the fermion models. A simple prescription has not yet been found, in contrast to the above-mentioned case at $T=0$.

Let us recall the quantum inverse scattering method based on the graded YB relation,[29,30] by which the integrability and other algebraic structures of the fermion systems have been discussed successfully.[29–35] This formulation has a severe problem when applied to the finite temperature case. We must treat the quantum and auxiliary spaces on the same footing when constructing the QTM. Conversely, in the graded YB relation the quantum space is the fermion Fock space, while the auxiliary space is the (graded) vector space.

To overcome these difficulties, we adopt another approach to fermion systems, which was invented quite recently.[36–38] In this method, we consider an R operator consisting of the fermion operators alone, together with its ''supertransposition.'' This time both quantum and auxiliary spaces are fermion Fock spaces. Therefore, we can, for instance, exchange their roles with no difficulty. Actually, by careful introduction of the supertrace and interchange of it with the normal trace to the partition function, we can derive a commuting QTM for the fermion systems.

The resultant QTM preserves genuine fermion statistics. In other words, the selection rule is already built in algebraically. This proper treatment of the statistics results in a change of the analytic structure for the QTM. In the ''physical strip,'' the QTM has only one additional zero which characterizes ''excited free energy'' at finite T, while in the corresponding spin model there appear two such zeros. Consequently, one observes a T-dependent oscillating behavior of one-particle Green's function, as well as the difference in the correlation length between the fermion model and the corresponding spin model. These are smoothly connected to the expected values at the conformal field theory (CFT) limit, $T\to 0$ (see Appendix B).

This paper is organized as follows. In Sec. II, we will present the commuting QTM formulation of the spinless fermion model at $T>0$. The fermionic R operator, together with its ''supertransposition'' $\widetilde{R}$, play fundamental roles. The analytic structure of the QTM and the auxiliary functions are discussed in Sec. III, which leads to the nonlinear integral equations (NLIE's) characterizing the correlation length. The limit $T\to 0$ is treated analytically at ''half-filling'' ($n_e=0.5$), which recovers the prediction from CFT. We also perform numerical investigations on NLIE's and the correlation length for one-particle Green's function. To our knowledge, this is the first exact computation of the correlation length for various interaction strengths, electron filling, and for a wide range of temperatures. In Sec. IV, we comment on alternative forms of NLIE's derived from different choice of the auxiliary functions. They are akin to the standard ''thermodynamic Bethe ansatz equations'' from the string hypothesis, and thus may be of interest in their own right. Details of calculations and supplementary knowledge on CFT are summarized in the appendixes.

II. COMMUTING QUANTUM TRANSFER MATRIX FOR THE SPINLESS FERMION MODEL

In this section we formulate the commuting QTM for the spinless fermion model. The formulation is based on recent developments in the study of the integrability of lattice fermion systems.[36–38] The central role is played by an operator solution of the YB equation called the fermionic R operator. The ''transfer matrix'' can be constructed from the R operator, which generates the left-shift operator, the fermionic Hamiltonian, and other conserved operators. Here and in Sec. II A, we briefly describe the method.

To extend the method to the finite temperature case utilizing the Trotter formula, it is necessary to look for another transfer matrix which generates the *right*-shift operator and the Hamiltonian. In Sec. II B, we shall argue how to construct the desired transfer matrix by considering the supertransposition of the R operator.

Based on these two kinds of the transfer matrices, we devise the QTM for the fermion model in Sec. II C. The QTM constitutes a one-parameter commuting family, which is a consequence of the global YB relation. The YB relation also enables us to diagonalize the QTM by means of the algebraic Bethe ansatz. The free energy and the correlation length are expressed in terms of the eigenvalues of the QTM.

A. Fermionic *R* Operator

We define the spinless fermion model by the Hamiltonian

$$\mathcal{H}:=\sum_{j=1}^{L}\mathcal{H}_{j,j+1}, \tag{2.1}$$

$$\mathcal{H}_{j,j+1}:=\frac{t}{2}\left\{c_j^{\dagger}c_{j+1}+c_{j+1}^{\dagger}c_j+2\Delta\left(n_j-\frac{1}{2}\right)\left(n_{j+1}-\frac{1}{2}\right)\right\},$$

where $c_j^{\dagger}$ and c_j are the fermionic creation and annihilation operators at the jth site satisfying the canonical anticommutation relations

$$\{c_j,c_k\}=\{c_j^{\dagger},c_k^{\dagger}\}=0,\quad \{c_j^{\dagger},c_k\}=\delta_{jk}. \tag{2.2}$$

We assume a periodic boundary condition (PBC) on the fermion operators,

$$c_{L+1}^{\dagger}=c_1^{\dagger},\quad c_{L+1}=c_1. \tag{2.3}$$

The parameters t and Δ are real coupling constants. In the present paper we consider the repulsive critical region $0\leqslant\Delta<1$, $0<t$, and introduce the parametrization

$$\Delta:=\cos 2\eta,\quad 0<2\eta\leqslant\frac{\pi}{2}. \tag{2.4}$$

In the subsequent sections, we shall also use the parameter p_0 defined by

$$p_0:=\frac{\pi}{2\eta}. \tag{2.5}$$

Hereafter we set $t=1$ for simplicity.

Model (2.1) is exactly solved by the Bethe ansatz method. Since the Hamiltonian (2.1) preserves the number of the particles, we can add the ''chemical potential'' term without breaking the integrability

$$\mathcal{H}_{\text{chemical}}:=\mu\sum_{j=1}^{L}\left(n_j-\frac{1}{2}\right). \tag{2.6}$$

We consider only the case $\mu=0$ for a while.

The several physical properties including the integrability of the fermion model (2.1) has been discussed by transforming it into the XXZ model

$$H=\frac{1}{4}\sum_{j=1}^{L}\{\sigma_j^x\sigma_{j+1}^x+\sigma_j^y\sigma_{j+1}^y+\Delta\sigma_j^z\sigma_{j+1}^z\} \qquad (2.7)$$

through the JW transformation. However, it was recently discovered that we can treat the fermion model (2.1) only with the fermion operators. We shall summarize the method in what follows.

First let us consider a two-dimensional fermion Fock space V_j, a basis of which is given by

$$|0\rangle_j, \quad |1\rangle_j := c_j^\dagger|0\rangle_j,$$
$$c_j|0\rangle_j=0. \qquad (2.8)$$

Define the fermionic R operator acting on the tensor product of the fermion Fock spaces $V_j\otimes_s V_k$ by

$$\mathcal{R}_{jk}(v):=a(v)\{-n_jn_k+(1-n_j)(1-n_k)\}+b(v)\{n_j(1-n_k)+(1-n_j)n_k\}+c(v)(c_j^\dagger c_k-c_jc_k^\dagger), \qquad (2.9)$$

where

$$a(v):=\frac{\sin\eta(v+2)}{\sin 2\eta}, \quad b(v):=\frac{\sin\eta v}{\sin 2\eta}, \quad c(v):=1. \qquad (2.10)$$

A basis of $V_j\otimes_s V_k$ is given by

$$|0\rangle_j\otimes_s|0\rangle_k:=|0\rangle, \quad |1\rangle_j\otimes_s|0\rangle_k:=c_j^\dagger|0\rangle,$$
$$|0\rangle_j\otimes_s|1\rangle_k:=c_k^\dagger|0\rangle, \quad |1\rangle_j\otimes_s|1\rangle_k:=c_j^\dagger c_k^\dagger|0\rangle, \qquad (2.11)$$

and we can calculate the matrix elements of Eq. (2.9) if necessary. We shall keep the operator form (2.9) as much as possible and avoid the use of the matrix elements, because the former is more transparent. The R operator (2.9) satisfies the YB equation[37,38]

$$\mathcal{R}_{12}(u-v)\mathcal{R}_{13}(u)\mathcal{R}_{23}(v)=\mathcal{R}_{23}(v)\mathcal{R}_{13}(u)\mathcal{R}_{12}(u-v). \qquad (2.12)$$

Equation (2.12) is an operator identity, and one should carefully use the anti-commutation relations (2.2) to confirm its validity.

It is one of the fundamental properties of the R operator $\mathcal{R}_{ij}(v)$ that $\mathcal{R}_{ij}(0)=\mathcal{P}_{ij}$ is the permutation operator for the fermion operators,

$$\mathcal{P}_{jk}:=(1-n_j)(1-n_k)-n_jn_k+c_j^\dagger c_k-c_jc_k^\dagger,$$
$$\mathcal{P}_{jk}x_j=x_k\mathcal{P}_{jk} \quad (x_j=c_j \quad \text{or} \quad c_j^\dagger). \qquad (2.13)$$

We can define an analog of the transfer matrix by

$$T(v):=\mathrm{Str}_a\{\mathcal{R}_{aL}(v)\cdots\mathcal{R}_{a1}(v)\}. \qquad (2.14)$$

Here the supertrace of an arbitrary operator X is defined by

$$\mathrm{Str}_aX:={}_a\langle 0|X|0\rangle_a-{}_a\langle 1|X|1\rangle_a, \qquad (2.15)$$

where the dual fermion Fock space is spanned by ${}_a\langle 0|$ and ${}_a\langle 1|$, with

$${}_a\langle 0|c_a^\dagger=0, \quad {}_a\langle 1|:={}_a\langle 0|c_a. \qquad (2.16)$$

We also assume

$${}_a\langle 0|0\rangle_a={}_a\langle 1|1\rangle_a=1. \qquad (2.17)$$

The supertrace (2.15) corresponds to the PBC for the fermion operators (2.3), thanks to the property

$$\mathrm{Str}_a\{\mathcal{R}_{aL}(v)\cdots\mathcal{R}_{a1}(v)\}=\mathrm{Str}_a\{\mathcal{R}_{a1}(v)\mathcal{R}_{aL}(v)\cdots\mathcal{R}_{a2}(v)\}. \qquad (2.18)$$

Hereafter we call Eq. (2.14) the transfer matrix for simplicity.

As in the case with the integrable spin models, the YB equation (2.12) ensures the commutativity of the transfer matrices (2.14),

$$[T(v),T(v')]=0. \qquad (2.19)$$

The expansion of the transfer matrix (2.15) with respect to the spectral parameter v is given by

$$T(v)=T(0)\left\{1+\frac{2\eta}{\sin 2\eta}\left(\mathcal{H}+\frac{L}{4}\Delta\right)v+O(v^2)\right\}, \qquad (2.20)$$

which follows from the relationship

$$\left.\frac{\mathrm{d}\mathcal{R}_{aj}(v)}{\mathrm{d}v}\right|_{v=0}\mathcal{P}_{a,j-1}=\frac{2\eta}{\sin 2\eta}\mathcal{P}_{aj}\mathcal{P}_{a,j-1}\left(\mathcal{H}_{j-1,j}+\frac{1}{4}\Delta\right). \qquad (2.21)$$

Note that the operator $T(0)=\mathrm{Str}_a\{\mathcal{P}_{aL}\cdots\mathcal{P}_{a1}\}$ is the left-shift operator,

$$T(0)x_j=x_{j+1}T(0) \quad (x_j=c_j \ \text{ or } \ c_j^\dagger). \qquad (2.22)$$

One can easily prove relation (2.22) utilizing the property of the permutation operator,

$$\mathcal{P}_{a,j+1}\mathcal{P}_{aj}\ x_j=x_{j+1}\mathcal{P}_{a,j+1}\mathcal{P}_{aj} \quad (x_j=c_j \ \text{ or } \ c_j^\dagger). \qquad (2.23)$$

B. Supertransposed fermionic R operator

In this section, we shall consider another transfer matrix which generates the right-shift operator. For this purpose we first define the super-transposition st_j for an arbitrary operator $X_j(v)$ in the form

$$X_j(v)=A(v)(1-n_j)+D(v)n_j+B(v)c_j+C(v)c_j^\dagger \qquad (2.24)$$

by

$$X_j^{\mathrm{st}_j}(v):=A(v)(1-n_j)+D(v)n_j+B(v)c_j^\dagger-C(v)c_j. \qquad (2.25)$$

Here $A(v)$ and $D(v)$ $[B(v)$ and $C(v)]$ are assumed to be Grassmann even (odd) operators.

Now applying the supertransposition st_1 to both sides of the YB equation (2.12), we obtain

$$\mathcal{R}^{st_1}_{13}(u)\mathcal{R}^{st_1}_{12}(u-v)\mathcal{R}_{23}(v)=\mathcal{R}_{23}(v)\mathcal{R}^{st_1}_{12}(u-v)\mathcal{R}^{st_1}_{13}(u), \tag{2.26}$$

where we have used a property of the supertransposition

$$[\mathcal{R}_{jk}(u)\mathcal{R}_{jl}(v)]^{st_j}=\mathcal{R}^{st_j}_{jl}(v)\mathcal{R}^{st_j}_{jk}(u) \quad (k\neq l). \tag{2.27}$$

Then changing suffixes and spectral parameters as

$$\begin{gathered}1\to 3,\quad 2\to 1,\quad 3\to 2,\\ u\to -v,\quad v\to u-v,\end{gathered} \tag{2.28}$$

we obtain the following type of the YB equation

$$\mathcal{R}_{12}(u-v)\tilde{\mathcal{R}}_{13}(u)\tilde{\mathcal{R}}_{23}(v)=\tilde{\mathcal{R}}_{23}(v)\tilde{\mathcal{R}}_{13}(u)\mathcal{R}_{12}(u-v), \tag{2.29}$$

where

$$\begin{aligned}\tilde{\mathcal{R}}_{jk}(v)&:=\mathcal{R}^{st_k}_{kj}(-v)=a(-v)\{-n_jn_k+(1-n_j)(1-n_k)\}\\ &+b(-v)\{n_j(1-n_k)+(1-n_j)n_k\}\\ &-c(-v)(c_j^\dagger c_k^\dagger+c_jc_k).\end{aligned} \tag{2.30}$$

Although the new R operator $\tilde{\mathcal{R}}_{jk}(v)$ is not symmetric $[\tilde{\mathcal{R}}_{jk}(v)\neq\tilde{\mathcal{R}}_{kj}(v)]$, it is still possible to prove the relation

$$\tilde{\mathcal{R}}_{12}(u-v)\tilde{\mathcal{R}}_{13}(u)\mathcal{R}_{23}(v)=\mathcal{R}_{23}(v)\tilde{\mathcal{R}}_{13}(u)\tilde{\mathcal{R}}_{12}(u-v). \tag{2.31}$$

Using $\tilde{\mathcal{R}}_{aj}(v)$, we define another transfer matrix by

$$\tilde{T}(v):=\mathrm{Str}_a\{\tilde{\mathcal{R}}_{aL}(v)\cdots\tilde{\mathcal{R}}_{a1}(v)\}. \tag{2.32}$$

Then the commutative properties of the transfer matrices follow from the YB equations (2.29) and (2.31),

$$[T(v),\tilde{T}(v')]=[\tilde{T}(v),\tilde{T}(v')]=0. \tag{2.33}$$

The relations

$$\tilde{\mathcal{P}}_{aj}\tilde{\mathcal{P}}_{a,j-1}x_j=x_{j-1}\tilde{\mathcal{P}}_{aj}\tilde{\mathcal{P}}_{a,j-1} \quad (x_j=c_j \text{ or } c_j^\dagger), \tag{2.34}$$

hold, where

$$\tilde{\mathcal{P}}_{jk}:=\tilde{\mathcal{R}}_{jk}(0)=(1-n_j)(1-n_k)-n_jn_k-(c_j^\dagger c_k^\dagger+c_jc_k). \tag{2.35}$$

Using relations (2.34), one can confirm that the operator $\tilde{T}(0)$ provides the right-shift operator, i.e.,

$$\tilde{T}(0)x_j=x_{j-1}\tilde{T}(0) \quad (x_j=c_j \text{ or } c_j^\dagger). \tag{2.36}$$

In other words, $\tilde{T}(0)$ is the inverse of $T(0)$,

$$T(0)\tilde{T}(0)=1. \tag{2.37}$$

Furthermore, from the relationship

$$\tilde{\mathcal{P}}_{a,j+1}\frac{d\tilde{\mathcal{R}}_{aj}(v)}{dv}\bigg|_{v=0}=-\frac{2\eta}{\sin 2\eta}\tilde{\mathcal{P}}_{a,j+1}\tilde{\mathcal{P}}_{aj}\left(\mathcal{H}_{j+1,j}+\frac{1}{4}\Delta\right), \tag{2.38}$$

the expansion of the transfer matrix $\tilde{T}(v)$ with respect to the spectral parameter v is given by

$$\tilde{T}(v)=\tilde{T}(0)\left\{1-\frac{2\eta}{\sin 2\eta}\left(\mathcal{H}+\frac{L}{4}\Delta\right)v+O(v^2)\right\}. \tag{2.39}$$

C. Commuting quantum transfer matrix

Expansions (2.20) and (2.39) with relation (2.37) are combined into a formula

$$T(u)\tilde{T}(-u)=1+\frac{4\eta}{\sin 2\eta}\left(\mathcal{H}+\frac{L}{4}\Delta\right)u+O(u^2). \tag{2.40}$$

This facilitates the investigation the finite temperature properties of the spinless fermion model (2.1) via the Trotter formula

$$\exp\left[-\beta\left(\mathcal{H}+\frac{L}{4}\Delta\right)\right]=\lim_{N\to\infty}[T(u_N)\tilde{T}(-u_N)]^{N/2},$$

$$u_N=-\frac{\beta\sin 2\eta}{2\eta N}. \tag{2.41}$$

Here an (even) integer N, called the Trotter number, represents the number of sites in the fictitious Trotter direction and β is the inverse temperature $\beta=1/T$.

The free energy per site, for instance, is given by

$$f=-\lim_{L\to\infty}\lim_{N\to\infty}\frac{1}{L\beta}\ln \mathrm{Tr}[T(u_N)\tilde{T}(-u_N)]^{N/2}-\frac{1}{4}\Delta. \tag{2.42}$$

However, as is the case with the corresponding spin model, the eigenvalues of $T(u_N)\tilde{T}(-u_N)$ are infinitely degenerate in the limit $N\to\infty$.

Therefore, it is a formidable task to take the trace in this limit. To avoid this difficulty, we transform the term $\mathrm{Tr}[T(u_N)\tilde{T}(-u_N)]^{N/2}$ in Eq. (2.42) as follows:

$$\begin{aligned}&\mathrm{Tr}[T(u_N)\tilde{T}(-u_N)]^{N/2}\\ &=\mathrm{Tr}\prod_{m=1}^{N/2}\mathrm{Str}_{a_{2m},a_{2m-1}}[\mathcal{R}_{a_{2m},L}(u_N)\cdots\mathcal{R}_{a_{2m},1}(u_N)\\ &\quad\times\tilde{\mathcal{R}}_{a_{2m-1},L}(-u_N)\cdots\tilde{\mathcal{R}}_{a_{2m-1},1}(-u_N)],\\ &=\mathrm{Str}\prod_{j=1}^{L}\mathrm{Tr}_j\prod_{m=1}^{N/2}\mathcal{R}_{a_{2m},j}(u_N)\tilde{\mathcal{R}}_{a_{2m-1},j}(-u_N).\end{aligned} \tag{2.43}$$

We now introduce a fundamental object in the present approach called the QTM

$$T_{\mathrm{QTM}}(u_N,v):=\mathrm{Tr}_j\,\mathcal{T}_j(u_N,v), \tag{2.44}$$

where the monodromy operator $\mathcal{T}_j(u_N,v)$ is defined by

$$\mathcal{T}_j(u_N,v):=\prod_{m=1}^{N/2}\mathcal{R}_{a_{2m},j}(v+u_N)\tilde{\mathcal{R}}_{a_{2m-1},j}(v-u_N). \tag{2.45}$$

Using the YB equations (2.12) and (2.29), we can show that the monodromy operator satisfies the global YB relation

$$\mathcal{R}_{21}(v-v')\mathcal{T}_1(u_N,v)\mathcal{T}_2(u_N,v') = \mathcal{T}_2(u_N,v')\mathcal{T}_1(u_N,v)\mathcal{R}_{21}(v-v'). \tag{2.46}$$

Accordingly the QTM constitutes a commuting family

$$[T_{\rm QTM}(u_N,v),T_{\rm QTM}(u_N,v')]=0. \tag{2.47}$$

We remark that the trace in the definition of the QTM (2.44) implies the antiperiodic boundary condition for the Fermion operators in the Trotter direction,[38] i.e.,

$$c_{a_{N+1}}=-c_{a_1}, \quad c^\dagger_{a_{N+1}}=-c^\dagger_{a_1}. \tag{2.48}$$

The free energy per site (2.42) is then represented in terms of the QTM as

$$f=-\lim_{L\to\infty}\lim_{N\to\infty}\frac{1}{L\beta}\ln {\rm Str}[T_{\rm QTM}(u_N,0)]^L-\frac{1}{4}\Delta. \tag{2.49}$$

Since the two limits in Eq. (2.49) are exchangeable,[5,6] we take the limit $L\to\infty$ first. Because there is a finite gap between the first and the second largest eigenvalue of the QTM for finite temperature, we can write

$$f=-\frac{1}{\beta}\lim_{N\to\infty}\ln\Lambda_1-\frac{1}{4}\Delta, \tag{2.50}$$

where Λ_1 is the first largest eigenvalue of the QTM, $T_{\rm QTM}(u_N,0)$. From now on Λ_k denotes the kth largest eigenvalue of the QTM. The correlation length ξ of the correlation function $\langle c_j^\dagger c_k\rangle$ can also be represented in terms of the first and second largest eigenvalues Λ_2 as

$$\xi^{-1}=-\lim_{N\to\infty}\ln\left|\frac{\Lambda_2}{\Lambda_1}\right|. \tag{2.51}$$

In this way the calculation of certain thermal quantities reduces to the evaluation of the eigenvalues of the QTM in the Trotter limit ($N\to\infty$).

For finite N, it is possible to diagonalize QTM (2.44) by means of the algebraic Bethe ansatz[39] (see Appendix A). The eigenvalue is then given by

$$\Lambda(x)=\lambda_1(x)+\lambda_2(x),$$

$$\lambda_1(x):=\phi_+(x)\phi_-(x-2i)\frac{Q(x+2i)}{Q(x)}e^{\beta\mu/2}, \tag{2.52}$$

$$\lambda_2(x):=(-1)^{N/2+N_e}\phi_-(x)\phi_+(x+2i)\frac{Q(x-2i)}{Q(x)}e^{-\beta\mu/2},$$

where

$$\phi_\pm(x):=\left(\frac{\sinh\eta(x\pm iu_N)}{\sin 2\eta}\right)^{N/2},$$

$$Q(x):=\prod_{j=1}^{N_e}\sinh\eta(x-x_j). \tag{2.53}$$

Here we have changed the spectral parameter from v to x defined by $v=ix$ for later convenience. Note that we have also included the contribution from the chemical potential term (2.6) in the expression (2.52).

The associated Bethe ansatz equation (BAE) is given by

$$\left(\frac{\phi_+(x)\phi_-(x-2i)}{\phi_-(x)\phi_+(x+2i)}\right)^{N/2} = -(-1)^{N/2+N_e}e^{-\beta\mu}\prod_{k=1}^{N_e}\frac{Q(x_j-2i)}{Q(x_j+2i)}. \tag{2.54}$$

Compared with the XXZ model, we observe an extra factor $(-1)^{N/2+N_e}$ in Eqs. (2.52) and (2.54) which reflects the fermionic nature of the present system. In particular, if $N/2+N_e\equiv 1 \pmod 2$, Eqs. (2.52) and (2.54) are clearly different from the corresponding ones for the XXZ model. Actually the second largest eigenvalue lies in the sector $N_e=N/2-1$, while the first largest one is in the sector $N_e=N/2$. Therefore, the correlation length ξ [Eq. (2.51)] exhibits the manifest difference between the fermion system (2.1) and the spin system (2.7).

III. NLIE AND THE EXACT ENUMERATION OF CORRELATION LENGTH

A. Analyticities of auxiliary functions and NLIE's

In order to proceed further, one needs to clarify the analytic property of the QTM. For this purpose, we perform numerical investigations by fixing the Trotter number N finite.

First we give the description for the largest eigenvalue sector, which is naturally identical to the corresponding XXZ model. There are $N_e=N/2$ BAE roots. Only at ''half-filling'' do they distribute exactly on the real axis symmetrically with respect to $x=0$, while for the general particle density they bend in the complex x plane. The QTM has N zeros in ${\rm Im}\,x\in[-p_0,p_0]$: $N/2$ zeros locate on the smooth curve ${\rm Im}\,x\sim 2$, and the other $N/2$ zeros are on the curve ${\rm Im}\,x\sim -2$. Thus there is a strip ${\rm Im}\,x\in[-1,1]$ where the QTM is analytic and nonzero. We call this the ''physical strip.''

Next consider the excited state relevant to the second largest eigenvalue. In contrast to the XXZ model, we find that two complex eigenvalues are degenerate in magnitude. Both of them are characterized by $N_e=N/2-1$ BAE roots located on a smooth curve near the real axis. The distribution of the BAE roots for the one and that for the other are symmetric with respect to the imaginary axis. As to the zeros of the QTM, $N-2$ zeros are on the smooth curves ${\rm Im}\,x\sim\pm 2$.

The locations of the two ''missing zeros'' are vital in the evaluation of the excited states. For the XXZ model, both of them enter into the physical strip. Especially with vanishing external field h, they are on the real axis and are symmetric with respect to the imaginary axis. With the increase of h,

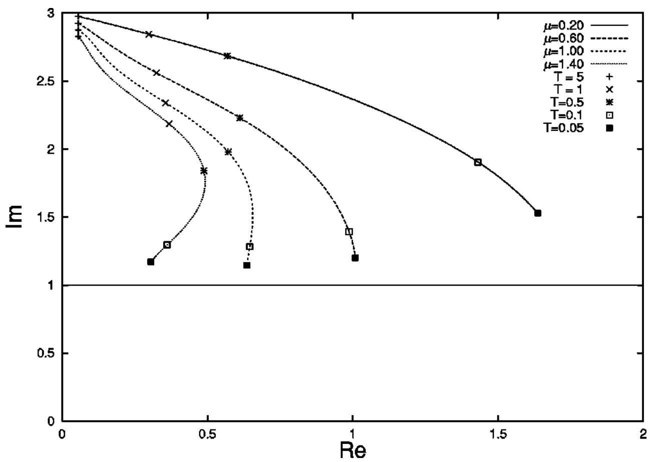

FIG. 1. The trajectories of the additional zero θ' are depicted in the cases $p_0=3$ and $N=100$. With the decrease of T, θ' moves downward, whereas it never comes into the physical strip.

they are away from the real axis, but still stay in the physical strip preserving the symmetry.

We find a different situation for the Fermion model. At half-filling, corresponding to $h=0$ in the XXZ model, one of them is located at θ_0 on the real axis, while the other is at $\theta_0'+ip_0$ and $\theta_0\sim\theta_0'$. That is, only one zero appears in the physical strip. Away from half-filling, the zero in the physical strip (we call it θ) moves upward while the other (θ') moves downward. Nevertheless, we find that θ remains in the physical strip while θ' never comes in. From now on we consider the case Re $\theta>0$ (Re $\theta'>0$). Then the trajectories of θ', for example, are depicted in Fig. 1.

We assume all these features are valid in the Trotter limit $N\to\infty$. Then a set of nonlinear integral equations can be derived as in the case of the XXZ model.[15] We define auxiliary functions

$$\mathfrak{a}(x):=\frac{\lambda_1(x+i-i\gamma_1)}{\lambda_2(x+i-i\gamma_1)},\quad \mathfrak{A}(x):=1+\mathfrak{a}(x),$$
$$\bar{\mathfrak{a}}(x):=\frac{\lambda_2(x-i+i\gamma_2)}{\lambda_1(x-i+i\gamma_2)},\quad \bar{\mathfrak{A}}(x):=1+\bar{\mathfrak{a}}(x). \tag{3,1}$$

where γ_1, and γ_2 are small positive quantities introduced for the convenience in numerical calculations. Note that these functions have asymptotic values

$$\mathfrak{a}(x)=\begin{cases}\exp((-\pi+4\eta)i+\beta\mu) & \text{for } x\to-\infty\\ \exp((\pi-4\eta)i+\beta\mu) & \text{for } x\to\infty,\end{cases} \tag{3.2a}$$

$$\bar{\mathfrak{a}}(x)=\begin{cases}\exp((\pi-4\eta)i-\beta\mu) & \text{for } x\to-\infty\\ \exp((-\pi+4\eta)i-\beta\mu) & \text{for } x\to\infty.\end{cases} \tag{3.2b}$$

Immediately seen from the above analyticity argument, $\mathfrak{a}(x),\mathfrak{A}(x)$ $[\bar{\mathfrak{a}}(x),\bar{\mathfrak{A}}(x)]$ are analytic, nonzero, and have constant asymptotic values (ANZC) in a certain strip in the lower (upper) half plane including real axis. The above definitions, together with the knowledge of zeros for $\Lambda(x)$, fix the NLIE among these auxiliary functions. We defer the detail derivation to Appendix C. The resultant expressions allow for taking the Trotter limit analytically. Thereby one arrives at the final expressions totally independent of fictitious parameter N,

$$\begin{aligned}\ln\mathfrak{a}(x)=&-\frac{\pi\beta\sin 2\eta}{4\eta\cosh\frac{\pi}{2}(x-i\gamma_1)}+F*\ln\mathfrak{A}(x)\\&-F*\ln\bar{\mathfrak{A}}(x+2i-i(\gamma_1+\gamma_2))\\&+2\pi i\mathcal{F}(x-\theta+i(1-\gamma_1))+\frac{\beta\mu p_0}{2(p_0-1)},\end{aligned} \tag{3.3}$$

$$\begin{aligned}\ln\bar{\mathfrak{a}}(x)=&-\frac{\pi\beta\sin 2\eta}{4\eta\cosh\frac{\pi}{2}(x+i\gamma_2)}+F*\ln\bar{\mathfrak{A}}(x)\\&-F*\ln\mathfrak{A}(x-2i+i(\gamma_1+\gamma_2))\\&-2\pi i\mathcal{F}(x-\theta-i(1-\gamma_2))-\frac{\beta\mu p_0}{2(p_0-1)}.\end{aligned}$$

where

$$A*B(x):=\int_{-\infty}^{\infty}A(x-y)B(y)dy,$$

$$F(x):=\frac{1}{2\pi}\int_{-\infty}^{\infty}\frac{\sinh(p_0-2)k}{2\cosh k\sinh(p_0-1)k}e^{-ikx}dk, \tag{3.4}$$

$$\mathcal{F}(x):=\frac{i}{2\pi}\int_{-\infty}^{\infty}\frac{\sinh(p_0-2)k}{2k\cosh k\sinh(p_0-1)k}e^{-ikx}dk.$$

Here, the integral in $\mathcal{F}(x)$ is the principal value. The location of zero θ satisfies a subsidiary condition

$$\mathfrak{a}(\theta-i+i\gamma_1)=-1. \tag{3.5}$$

Taking the Trotter limit $N\to\infty$ after setting $x=0$ in Eq. (C13), we derive that the "first excited free energy" per site f_2 is

$$\begin{aligned}f_2=&-\frac{1}{\beta}\ln\Lambda_2(0)-\frac{1}{4}\Delta=\epsilon_0-\frac{1}{\beta}K*\ln\mathfrak{A}(i\gamma_1)\\&-\frac{1}{\beta}K*\ln\bar{\mathfrak{A}}(-i\gamma_2)-\frac{1}{\beta}\ln\tanh\frac{\pi\theta}{4}-i\frac{\pi}{2\beta},\end{aligned} \tag{3.6}$$

where ϵ_0 is the ground-state energy defined in Eq. (C20) and

$$K(x):=\frac{1}{4\cosh\frac{\pi x}{2}}. \tag{3.7}$$

Together with the NLIE for the largest eigenvalue, summarized in Appendix C, these relations characterize the correlation length ξ of one-particle Green's function $\langle c_j^\dagger c_i\rangle$ at $T>0$ completely [see Eq. (2.51)].

We remark that in derivations of above relations one does not need precise information like roots distributions of the BAE. Only ANZC properties of the QTM and the auxiliary functions are sufficient. Thus the structure is rather robust, and permits one to introduce small free parameters γ_1 and γ_2. In the next two subsections, we present analytical and numerical studies on these equations and the correlation length of one-particle Green's function, which are main results in this paper.

B. Low temperature property of NLIE $(\mu=0)$

We study the low-temperature behavior for the half-filling case $\mu=0$ utilizing the dilogarithm trick,[40] which enables us to obtain the first low temperature correction without solving the NLIE. As in the case of the largest eigenvalue sector, $|\mathfrak{a}(x)|$ and $|\bar{\mathfrak{a}}(x)|$ exhibit a crossover behavior

$$\begin{aligned}|\mathfrak{a}(x)|,|\bar{\mathfrak{a}}(x)|&\ll 1 \quad \text{for } |x|<\mathcal{K},\\ |\mathfrak{a}(x)|,|\bar{\mathfrak{a}}(x)|&\sim 1 \quad \text{for } |x|>\mathcal{K},\end{aligned} \tag{3.8}$$

where

$$\mathcal{K}:=\frac{2}{\pi}\ln\frac{\pi\beta\sin(2\eta)}{2\eta}. \tag{3.9}$$

Thus one carefully takes into account of contributions near ''Fermi surfaces' $\pm\mathcal{K}$. For this purpose, we introduce the shifted variables and scaling functions

$$\begin{aligned}la_{\pm}(x)&:=\ln\mathfrak{a}\left(\pm\frac{2}{\pi}x\pm\mathcal{K}\right),\\ l\bar{a}_{\pm}(x)&:=\ln\bar{\mathfrak{a}}\left(\pm\frac{2}{\pi}x\pm\mathcal{K}\right),\\ \bar{\theta}&:=\frac{\pi}{2}(\theta-\mathcal{K}).\end{aligned} \tag{3.10}$$

and similarly for capital functions $\mathfrak{A}$, $\bar{\mathfrak{A}}$, $A_{\pm}$, and $\bar{A}_{\pm}$. In $T\to 0$, these satisfy the truncated equations

$$\begin{aligned}la_{+}(x)=&-e^{-x+(\pi/2)i\gamma_1}+F_1*lA_{+}(x)-F_2*l\bar{A}_{+}(x)\\ &+2\pi i\mathcal{F}\left(\frac{2}{\pi}(x-\bar{\theta})+i(1-\gamma_1)\right),\end{aligned} \tag{3.11a}$$

$$\begin{aligned}l\bar{a}_{+}(x)=&-e^{-x-(\pi/2)i\gamma_2}+F_1*l\bar{A}_{+}(x)-\bar{F}_2*lA_{+}(x)\\ &-2\pi i\mathcal{F}\left(\frac{2}{\pi}(x-\bar{\theta})-i(1-\gamma_2)\right),\end{aligned} \tag{3.11b}$$

$$\begin{aligned}la_{-}(x)=&-e^{-x-(\pi/2)i\gamma_1}+F_1*lA_{-}(x)-\bar{F}_2*l\bar{A}_{-}(x)\\ &+2\pi i\mathcal{F}(-\infty),\end{aligned} \tag{3.11c}$$

$$\begin{aligned}l\bar{a}_{-}(x)=&-e^{-x+(\pi/2)i\gamma_2}+F_1*l\bar{A}_{-}(x)-F_2*lA_{-}(x)\\ &-2\pi i\mathcal{F}(-\infty),\end{aligned} \tag{3.11d}$$

where

$$\begin{aligned}F_1(x)&:=\frac{2}{\pi}F\left(\frac{2x}{\pi}\right),\\ F_2(x)&:=\frac{2}{\pi}F\left(\frac{2}{\pi}x+2i-i(\gamma_1+\gamma_2)\right).\end{aligned} \tag{3.12}$$

and $\bar{F}_1$ and $\bar{F}_2$ are their complex conjugate. In this limit, the finite T correction part, $\ln\Lambda_{\text{fn}}(x)$ [see Eq. (C14b)] reads

$$\begin{aligned}\ln\Lambda_{\text{fn}}(x)\sim\frac{\pi}{2}i+\frac{2\eta}{\pi^2\beta\sin 2\eta}\Bigg(&-2\pi e^{(\pi/2)x-\bar{\theta}}\\ &+e^{(\pi/2)x}\int_{-\infty}^{\infty}e^{-y}\{e^{(\pi/2)i\gamma_1}lA_{+}(y)\\ &+e^{-(\pi/2)i\gamma_2}l\bar{A}_{+}(y)\}dy\\ &+e^{-(\pi/2)x}\int_{-\infty}^{\infty}e^{-y}\{e^{-(\pi/2)i\gamma_1}lA_{-}(y)\\ &+e^{(\pi/2)i\gamma_2}l\bar{A}_{-}(y)\}dy\Bigg).\end{aligned} \tag{3.13}$$

Thanks to the subsidiary condition for the additional zero θ [Eq. (3.5)], we have

$$\begin{aligned}e^{-\bar{\theta}}=\pi-\frac{2i}{\pi}\Bigg[&\int_{-\infty}^{\infty}F\left(\frac{2}{\pi}(z-\bar{\theta})+i(1-\gamma_1)\right)lA_{+}(z)dz\\ &-\int_{-\infty}^{\infty}F\left(\frac{2}{\pi}(z-\bar{\theta})-i(1-\gamma_2)\right)l\bar{A}_{+}(z)dz\Bigg].\end{aligned} \tag{3.14}$$

For further simplification, we define $D_{\pm}$ by

$$\begin{aligned}D_{\pm}:=&\int_{-\infty}^{\infty}\Bigg(lA_{\pm}(x)\frac{d}{dx}la_{\pm}(x)+l\bar{A}_{\pm}(x)\frac{d}{dx}l\bar{a}_{\pm}(x)\\ &-la_{\pm}(x)\frac{d}{dx}lA_{\pm}(x)-l\bar{a}_{\pm}(x)\frac{d}{dx}l\bar{A}_{\pm}(x)\Bigg)dx\\ =&\int_{a_{\pm}(-\infty)}^{a_{\pm}(\infty)}\left(\frac{\ln(1+a)}{a}-\frac{\ln a}{1+a}\right)da\\ &+\int_{\bar{a}_{\pm}(-\infty)}^{\bar{a}_{\pm}(\infty)}\left(\frac{\ln(1+\bar{a})}{\bar{a}}-\frac{\ln\bar{a}}{1+\bar{a}}\right)d\bar{a}.\end{aligned} \tag{3.15}$$

Obviously, they are equal to special values of Roger's dilogarithm $\mathcal{L}$,

$$\begin{aligned}D_{\pm}=&2\mathcal{L}\left(\frac{a_{\pm}(\infty)}{1+a_{\pm}(\infty)}\right)+2\mathcal{L}\left(\frac{\bar{a}_{\pm}(\infty)}{1+\bar{a}_{\pm}(\infty)}\right)\\ &-2\mathcal{L}\left(\frac{a_{\pm}(-\infty)}{1+a_{\pm}(-\infty)}\right)-2\mathcal{L}\left(\frac{\bar{a}_{\pm}(-\infty)}{1+\bar{a}_{\pm}(-\infty)}\right),\end{aligned} \tag{3.16}$$

$$\mathcal{L}(x):=-\frac{1}{2}\int_0^x dy\left[\frac{\ln(1-y)}{y}+\frac{\ln y}{1-y}\right].$$

We then apply the dilogarithm trick to Eqs. (3.11a)–(3.11d). For example, we take the first two equations. After differentiating, we multiply them by $lA_{+}(x)$ and $l\bar{A}_{+}(x)$, respectively, and take the summation. We call resultant equality

(A). Next multiply Eqs. (3.11a) and (3.11b) by $[l A_+(x)]'$ and $[l\overline{A}_+(x)]'$, respectively, and take the summation. Let us call the outcome (B). Finally we subtract (B) from (A) and integrate over x. The left-hand side of the equality is nothing but D_+. Remarkably on the right-hand side, most complicated terms like

$$-\int lA_+(x)\frac{dF_2(x-y)}{dx}l\overline{A}_+(y)dx\,dy$$
$$=-\int lA_+(x)F_2(x-y)\frac{dl\overline{A}_+(y)}{dy}dx\,dy, \qquad (3.17)$$

and

$$\int \frac{dl\overline{A}_+(x)}{dx}\overline{F}_2(x-y)lA_+(y)dx\,dy, \qquad (3.18)$$

cancel each other. After rearrangement, we obtain

$$D_+ + 2\pi i\mathcal{F}(\infty)\ln\frac{A_+(\infty)}{\overline{A}_+(\infty)}$$
$$=\int_{-\infty}^{\infty}2e^{-y}[e^{(\pi/2)i\gamma_1}lA_+(y)+e^{-(\pi/2)i\gamma_2}l\overline{A}_+(y)]dy$$
$$+8i\int_{-\infty}^{\infty}F\left(\frac{2}{\pi}(x-\overline{\theta})+i(1-\gamma_1)\right)lA_+(x)dx$$
$$-8i\int_{-\infty}^{\infty}F\left(\frac{2}{\pi}(x-\overline{\theta})-i(1-\gamma_2)\right)l\overline{A}_+(x)dx, \qquad (3.19)$$

where $a_+(-\infty)=\overline{a}_+(-\infty)=0$ is used. Similarly, from Eq. (3.11c) and (3.11d), we have

$$D_- + 2\pi i\mathcal{F}(-\infty)\ln\frac{A_-(\infty)}{\overline{A}_-(\infty)}=\int_{-\infty}^{\infty}2e^{-y}[e^{-(\pi/2)i\gamma_1}lA_-(y)$$
$$+e^{(\pi/2)i\gamma_2}l\overline{A}_-(y)]dy, \qquad (3.20)$$

Applying Eqs. (3.19) and (3.20), together with Eqs. (3.14), to Eq. (3.13),

$$\ln\Lambda_{\mathrm{fn}}(x)\sim\frac{\pi}{2}i+\frac{2\eta}{2\pi^2\beta\sin 2\eta}\Bigg\{e^{(\pi/2)x}\Bigg(-4\pi^2+D_+$$
$$+2\pi i\mathcal{F}(\infty)\ln\frac{A_+(\infty)}{\overline{A}_+(\infty)}\Bigg)$$
$$+e^{-\pi x/2}\Bigg(D_-+2\pi i\mathcal{F}(-\infty)\ln\frac{A_-(\infty)}{\overline{A}_-(\infty)}\Bigg)\Bigg\}. \qquad (3.21)$$

Now that the asymptotic values are easily found,

$$\mathcal{F}(\infty)=-\mathcal{F}(-\infty)=\frac{\pi-4\eta}{4(\pi-2\eta)},$$
$$a_+(\infty)=\overline{a}_-(\infty)=e^{(\pi-4\eta)i}, \qquad (3.22)$$
$$a_-(\infty)=\overline{a}_+(\infty)=e^{(-\pi+4\eta)i},$$

we can explicitly evaluate Eq. (3.21) at $x=0$,

$$\ln\Lambda_{\mathrm{fn}}(x=0)=\frac{\pi}{6\beta v_F}-\frac{\pi}{\beta v_F}\left(\frac{1}{\alpha}+\frac{\alpha}{4}\right)+\frac{\pi}{2}i, \qquad (3.23)$$

where $\mathcal{L}(x)+\mathcal{L}(1-x)=\pi^2/6$ is also applied. Here α is introduced in Eq. (B6) and the Fermi velocity v_F is also derived in Eq. (B13) for $n_e=0.5$. The first term is identical to the largest eigenvalue sector, and it reproduces a conformal anomaly term with $c=1$. Comparing them, one concludes that

$$\frac{\Lambda_2}{\Lambda_1}\sim e^{ik_F-1/\xi}, \qquad (3.24)$$

where k_F denotes the ''Fermi momentum.'' Note that $k_F=\pi/2$ in the half-filling case. Consequently the inverse correlation length is given as

$$\xi^{-1}=\frac{\pi T}{v_F}\left(\frac{1}{\alpha}+\frac{\alpha}{4}\right), \qquad (3.25)$$

These are nothing but the expected results from CFT [see Eq. (B14)]. This fact represents the consistency of both our result and validity of CFT mapping in the finite-temperature problem at low temperatures.

C. Numerical analyses on NLIE's

Having verified consistency at the specific limits, we now perform numerical analyses on the NLIE's for a wide range of temperatures, electron fillings, and interaction strengths. To keep the electron filling constant, we adopt the temperature-dependent chemical potential which are determined by the curve

$$\frac{d\langle n_e(T,\mu(T))\rangle}{dT}=\frac{d}{dT}\left(\frac{\partial f}{\partial\mu}\right)_T=0. \qquad (3.26)$$

The NLIE's are numerically solved by the iteration method. In each iteration steps, convolution parts are treated by the fast fourier transformation (FFT). As a technical remark, we call an attention to proper re-scaling of auxiliary functions for the FFT; one needs to modify the integrands such that these asymptotic values vanish. From the asymptotics in Eqs. (3.2a) and (3.2b), we introduce

$$\mathfrak{B}(x):=\begin{cases}\mathfrak{A}(x)/\mathfrak{A}(\infty) & \text{for } x\geq 0\\ \mathfrak{A}(x)/\mathfrak{A}(-\infty) & \text{for } x<0,\end{cases} \qquad (3.27)$$

and similarly for others. We also rewrite the NLIE's in terms of $\mathfrak{B}(x)$, which now has zero asymptotic values. For example,

$$
\begin{aligned}
\ln \mathfrak{a}(x) = & -\frac{\pi\beta \sin(2\eta)}{4\eta\cosh\frac{\pi}{2}(x-i\gamma_1)} + F*\ln \mathfrak{B}(x) \\
& - F*\ln \bar{\mathfrak{B}}(x+2i-i(\gamma_1+\gamma_2)) + \mathcal{F}(x)\ln\frac{\mathfrak{A}(\infty)}{\mathfrak{A}(-\infty)} \\
& - \mathcal{F}(x+2i-i(\gamma_1+\gamma_2))\ln\frac{\bar{\mathfrak{A}}(\infty)}{\bar{\mathfrak{A}}(-\infty)} \\
& + 2\pi i \mathcal{F}(x-\theta+i(1-\gamma_1)) + \beta\mu. \qquad (3.28)
\end{aligned}
$$

In addition, one must be careful in the branch cuts of the logarithms. In the above, $\ln \mathfrak{A}(\infty)/\mathfrak{A}(-\infty)$ and so on must be understood as

$$
\ln\frac{\mathfrak{A}(\infty)}{\mathfrak{A}(-\infty)} = \ln\left(-\frac{\sinh(\beta\mu/2-2i\eta)}{\sinh(\beta\mu/2+2i\eta)}\right) + (\pi-4\eta)i. \qquad (3.29)
$$

Under these arrangements, the iteration method works in a stable manner. We plot the temperature dependence of the correlation length ξT in Fig. 2 for various fillings keeping the interaction strength constant $\Delta=\cos(\pi/6)$.

The extrapolated values $T\to 0$ agree with the predictions from CFT within a few percent, even far away from ''half-filling'' ($n_e=0.5$). The curves are going down gradually with the decrease of electron density n_e. As further information, the chemical potential $\mu(T)$ determined by Eq. (3.26) and the locations of the additional zero θ are depicted in Figs. 3 and 4, respectively. The zero θ moves on a smooth curve and its curvature increases with the decrease of n_e. In fact, we find that it moves to $\theta=i$ when $n_e, T\to 0$. (See also the analytic argument for the noninteracting fermion case in Fig. 10 for $\mu=1.0$.) We also calculate the ''Fermi momentum'' $k_{\rm F}=\operatorname{Im}\ln \Lambda_2/\Lambda_1$ [cf. Eq. (3.24)]. (Here the inverse period of oscillatory behavior at arbitrary T is referred to as k_F as in the case of $T=0$.) The figure clearly shows the temperature dependency of k_F. In the low-temperature limit $T\to 0$, it converges to the expected value $k_F=n_e\pi$, which indicates the significance of the Fermi surface for one-particle excitations in the Luttinger liquid at $T=0$.[41] With the increase of T, the auxiliary functions cease to exhibit a sharp crossover behavior [Eq. (3.8)], which roughly corresponds to a broadening of the Fermi distribution at $T>0$. The particle excitations are enhanced within the wide range near the Fermi surface, which yield the shift of k_F (see Fig. 5). We remark that such a T-dependent oscillatory behavior has been reported for the longitudinal correlation function of ferromagnetic Heisenberg model.[24] Although physical origins are different for these two cases, the explicit determination of T dependency is important.

Figures 6 and 7 present the temperature dependence of the correlation length for various interaction strengths for fixed n_e. Naturally in the limit $n_e, T\to 0$, ξT does not depend significantly on the interaction strength; it merely behaves as $\xi T \sim v_F/\pi \sim n_e$ (see Appendix B). This fact is typical for noninteracting cases. Although our model inherits strong correlations, Fig. 6 indicates that $n_e=0.1$ is already well described by the ''noninteracting approximation,'' and also shows that this approximation is applicable in the wide range of T. On the other hand, data for $n_e=0.4$ show a strong dependency on Δ; therefore $n_e=0.4$ belongs to proper ''interacting class'' (see Fig. 7). It seems this crossover occurs near $n_e\sim 0.25$, but it is not yet conclusive. We hope to clarify this in a future communication.

Finally we plot the correlation length of the transverse spin-spin correlation $\langle \sigma_j^+ \sigma_j^- \rangle$ without external field (Fig. 8) for comparison with $n_e=0.5$ of spinless fermion models (Fig. 9). In addition to the difference between their limiting values at $T\to 0$, one clearly sees the difference in the dependence of ξT on T.

IV. SUMMARY AND DISCUSSION

We have proposed the QTM approach to integrable lattice fermion systems at any finite temperatures. The fermionic R operator, together with its supertransposition $\widetilde{R}$, where the fermion statistics is embedded naturally, play the crucial role in this approach. Consequently, we have observed a significant difference between the fermion model and that of the spin model. In principle, we can apply this approach to any integrable 1D fermion systems. The application to the Hubbard model is in progress.

Here we comment on the ''attractive regime'' $t>0$, $\Delta<0$ in Eq. (2.1), which we have not been concerned with in this paper. In the XXZ model without an external magnetic field, one may recall the remarkable difference between the repulsive (antiferromagnetic) case and the attractive (ferromagnetic) one.[23,24] In the repulsive regime, the eigenvalues related to the correlation $\langle \sigma_j^+ \sigma_i^- \rangle$ or $\langle \sigma_j^z \sigma_i^z \rangle$ are characterized by two real additional zeros which are symmetric with respect to the imaginary axis. This symmetry is never broken at any temperatures. On the other hand, in the attractive regime, ''level crossing'' occurs successively. One may attribute this to the change of the distribution patterns of the additional zeros. It will be interesting to see if similar phenomena occur for the spinless fermion model in the attractive regime.

Finally we refer to another formulation of NLIE's derived from the different choice of the auxiliary functions. The NLIE's have a close connection with the ''TBA'' or ''excited-states TBA'' equations from the standard ''string hypothesis.''

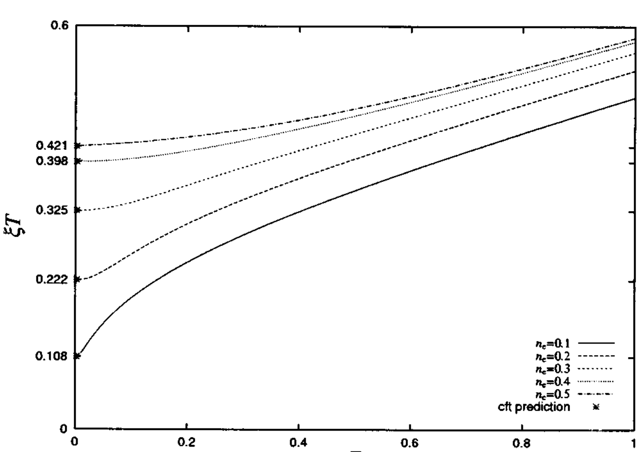

FIG. 2. The temperature dependence of the correlation length ξ for $p_0=6$.

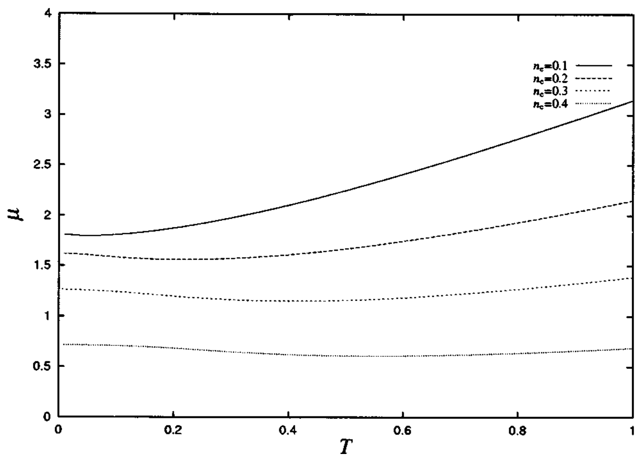

FIG. 3. The temperature dependence of the chemical potential μ for $p_0=6$.

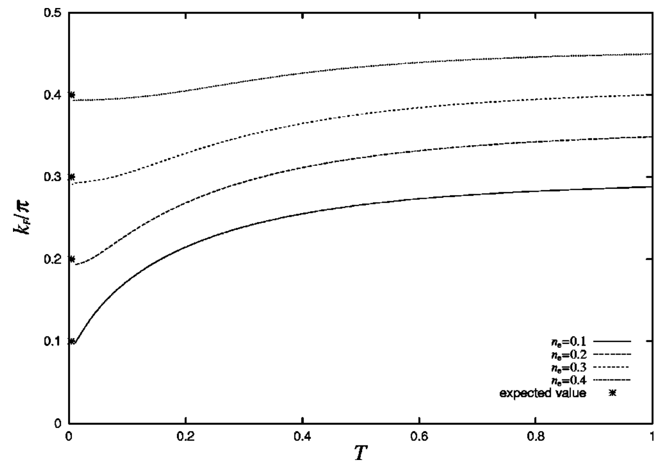

FIG. 5. The temperature dependence of the Fermi momentum k_F for $p_0=6$.

The idea is as follows. First we embed the QTM itself into a more general family called T functions, and explore functional relations among them (T systems). Then we define the Y functions by a certain ratio of the T functions, and also derive functional relations for them (the Y system). The analytical properties of these functions lead to the NLIE's which determine the free energy and the correlation length. As concerns the largest eigenvalue sector, the T functions coincide with those in Ref. 21. Therefore the derived NLIE's for the free energy are identical to the TBA equations of the XXZ model.[4,21] In contrast, for the second-largest eigenvalue sector we find the essential difference between the fermion model and the corresponding spin model. For example, we explicitly write the NLIE's (is the excited-state TBA equations) for $p_0=5$ and $\mu=0$ as

$$\ln\eta_1(x)=-\frac{5\beta\sin\frac{\pi}{5}x}{2\cosh\frac{\pi}{2}x}+K*\ln(1+\eta_2)(x)+\pi i,$$

$$\ln\eta_2(x)=K*\ln(1-\eta_1)(1-\eta_3)(x)+\ln\left(\tanh\frac{\pi}{4}(x-\theta_1)\tanh\frac{\pi}{4}(x-\theta_2)\right)+\pi i, \tag{4.1}$$

$$\ln\eta_3(x)=K*\ln(1+\eta_2)(1-\kappa^2)(x),$$

$$\ln\kappa=K*\ln(1-\eta_2)(x)+\ln\left(\tanh\frac{\pi}{4}(x-\theta_2)\right)+\frac{\pi}{2}i,$$

where θ_1 and θ_2 are determined from

$$i\frac{5\beta\sin\frac{\pi}{5}\theta_1}{2\sinh\frac{\pi}{2}\theta_1}+K*\ln(1+\eta_2)(\theta_1+i)-\pi i=0,$$

$$K*\ln(1+\eta_2)(1-\kappa^2)(\theta_2+i)=0. \tag{4.2}$$

The meaning of the functions η_j and the quantities θ_j are similar to those in Ref. 21. Although the above expressions are quite different from those in Sec. III, the numerical result

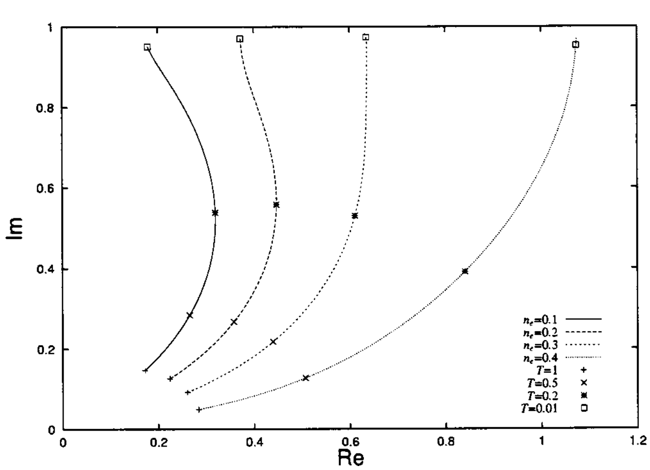

FIG. 4. The trajectory of the additional zero θ inside the physical strip.

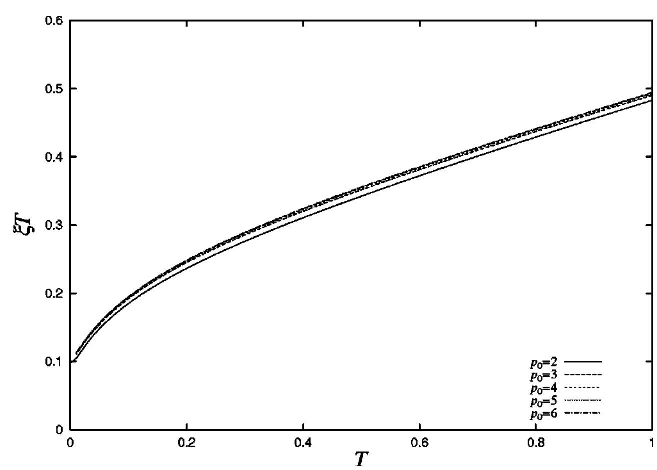

FIG. 6. The temperature dependence of the correlation length for $n_e=0.1$.

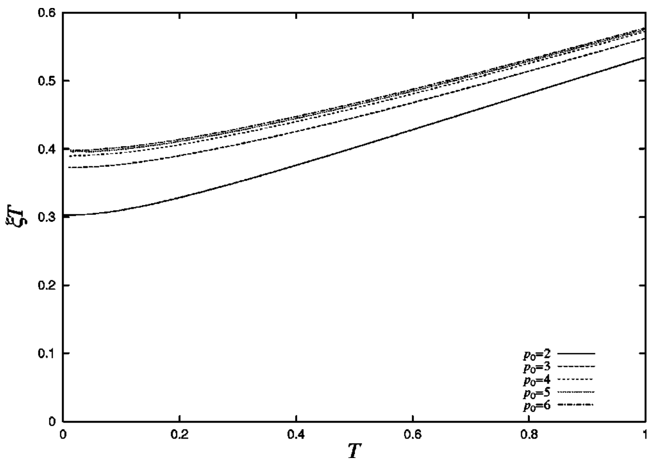

FIG. 7. The temperature dependence of the correlation length for $n_e = 0.4$.

shows a good agreement. The detailed derivations of above equations will be described in a separate communication.[42]

ACKNOWLEDGMENTS

The authors are grateful to A. Kuniba and M. Wadati for helpful comments and continuous encouragement. M.S. thanks H. Asakawa for discussions. J.S. thanks A. Klümper, R. Martinez, B. M. McCoy, and C. Scheeren for useful discussions. This work was in part supported by a Grant-in-Aid from the Ministry of Education, Science, Sports and Culture of Japan.

APPENDIX A: DIAGONALIZATION OF THE QUANTUM TRANSFER MATRIX

Here we shall diagonalize the QTM (2.44) by means of the algebraic Bethe ansatz. First let us recall that the monodromy operator (2.45) satisfies the global Yang-Baxter relation

$$\mathcal{R}_{21}(v-v')\mathcal{T}_1(u_N,v)\mathcal{T}_2(u_N,v') = \mathcal{T}_2(u_N,v')\mathcal{T}_1(u_N,v)\mathcal{R}_{21}(v-v'). \tag{A1}$$

Writing the monodromy operator as

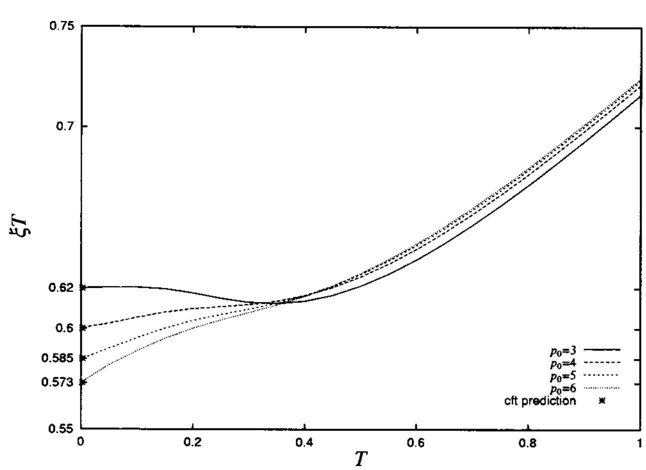

FIG. 8. The correlation length for $\langle \sigma_j^+ \sigma_i^- \rangle$ of the corresponding XXZ model with zero magnetic field.

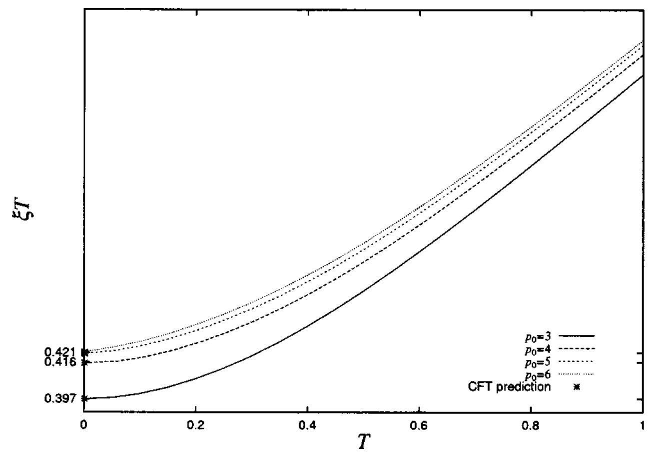

FIG. 9. The temperature dependence of the correlation length at half-filling.

$$\mathcal{T}_j(u_N,v) = A(v)(1-n_j) + B(v)c_j + C(v)c_j^\dagger + D(v)n_j, \quad j=1,2, \tag{A2}$$

and substituting this into Eq. (A1), we obtain the commutation relations among the operators $A(v),\ldots,D(v)$,

$$A(v)B(v') = \frac{a(v'-v)}{b(v'-v)}B(v')A(v) - \frac{c(v'-v)}{b(v'-v)}B(v)A(v'), \tag{A3a}$$

$$D(v)B(v') = -\frac{a(v-v')}{b(v-v')}B(v')D(v) + \frac{c(v-v')}{b(v-v')}B(v)D(v'), \tag{A3b}$$

$$B(v)B(v') = B(v')B(v). \tag{A3c}$$

To derive these relations, one should pay attention to the fact that $B(v)$ and $C(v)$ anti-commute with the Fermion operators c_j and $c_j^\dagger$.

The commutation relations (A3a)–(A3c) are quite similar to the corresponding ones for the XXZ model.[39] In fact, relations (A3a) and (A3c) are identical. The second relation (A3b), however, is different: there appears an overall ''minus'' sign on the right-hand side

Now we define the reference state by

$$|\Omega\rangle := \prod_{m=1}^{N/2} |0\rangle_{a_{2m}} \otimes_s |1\rangle_{a_{2m-1}}, \qquad |1\rangle_{a_{2m-1}} := c^\dagger_{a_{2m-1}}|0\rangle_{a_{2m-1}}. \tag{A4}$$

Then, using the relations

$$\tilde{R}_{a_{2m-1},j}(v-u_N)|1\rangle_{a_{2m-1}} = -a(-v+u_N)n_j|1\rangle_{a_{2m-1}} + b(-v+u_N)(1-n_j)|1\rangle_{a_{2m-1}} + c_j|0\rangle_{a_{2m-1}} \tag{A5}$$

and

$$R_{a_{2m},j}(v+u_N)|0\rangle_{a_{2m}}=a(v+u_N)(1-n_j)|0\rangle_{a_{2m}} +b(v+u_N)n_j|0\rangle_{a_{2m}}-c_j|1\rangle_{a_{2m}}, \tag{A6}$$

we find that

$$A(v)|\Omega\rangle=(a(v+u_N)b(-v+u_N))^{N/2}|\Omega\rangle, \tag{A7}$$

$$D(v)|\Omega\rangle=(-b(v+u_N)a(-v+u_N))^{N/2}|\Omega\rangle. \tag{A8}$$

Hence the state $|\Omega\rangle$ is an eigenstate of the QTM (2.44) with the eigenvalue

$$\Lambda_0(v)=\left(\frac{\sin\eta(v+u_N+2)\sin\eta(-v+u_N)}{\sin^2 2\eta}\right)^{N/2} +\left(-\frac{\sin\eta(v+u_N)\sin\eta(-v+u_N+2)}{\sin^2 2\eta}\right)^{N/2}. \tag{A9}$$

An eigenstate with N_e ''particles'' can be constructed by multiplying the operators $B(v_j)$ to the reference state

$$|\Psi\rangle:=\prod_{j=1}^{N_e} B(v_j)|\Omega\rangle. \tag{A10}$$

Indeed, using the standard argument of the algebraic Bethe ansatz,[39] we can show that state (A10) becomes the eigenstate of the QTM if the spectral parameters v_j fulfill the Bethe ansatz equations

$$\left[\frac{\sin\eta(-v_j+u_N)\sin\eta(v_j+u_N+2)}{\sin\eta(v_j+u_N)\sin\eta(-v_j+u_N+2)}\right]^{N/2} =-(-1)^{N/2+N_e}\prod_{k=1}^{N_e}\frac{\sin\eta(v_j-v_k+2)}{\sin\eta(v_j-v_k-2)}. \tag{A11}$$

The corresponding eigenvalue of the QTM (2.44),

$$T_{\mathrm{QTM}}(u_N,v)|\Psi\rangle=\Lambda(v)|\Psi\rangle, \tag{A12}$$

is given by

$$\Lambda(v)=\left(\frac{\sin\eta(v+u_N+2)\sin\eta(-v+u_N)}{\sin^2 2\eta}\right)^{N/2} \times\prod_{j=1}^{N_e}\frac{\sin\eta(v-v_j-2)}{\sin\eta(v-v_j)}+(-1)^{N/2+N_e} \times\left(\frac{\sin\eta(v+u_N)\sin\eta(-v+u_N+2)}{\sin^2 2\eta}\right)^{N/2} \times\prod_{j=1}^{N_e}\frac{\sin\eta(v-v_j+2)}{\sin\eta(v-v_j)}. \tag{A13}$$

APPENDIX B: $T\ll 1$ BEHAVIOR AND PREDICTION FROM CFT

We summarize the known results of the correlation function at $T=0$ and its $T\ll 1$ behavior predicted from CFT.[39,41] Let us start with the zero-temperature case. The one-particle Green's function shows an oscillatory behavior due to the Fermi surface,[41]

$$\langle c^\dagger(x)c(0)\rangle\sim\cos(k_F x)/x^{2\triangle}. \tag{B1}$$

The scaling dimension $\triangle$ is evaluated from the energy spectra in the finite-size system,

$$\triangle=\frac{1}{4Z(\mathcal{K}_F)^2}(\triangle N)^2+Z(\mathcal{K}_F)^2(\triangle D)^2. \tag{B2}$$

Here $Z(\mathcal{K}_F)$ is the dressed charge, and $\mathcal{K}_F$ denotes the ''Fermi surface'' satisfying

$$Z(x)+\frac{1}{2\pi}\int_{-\mathcal{K}_F}^{\mathcal{K}_F}R(x-y)Z(y)dy=1, \qquad R(x)=\frac{2\sin 4\eta}{\cosh 2x-\cos 4\eta}. \tag{B3}$$

$\triangle D$ and $\triangle N$ are (half-)integers constrained by a selection rule, $\triangle D=\triangle N/2 \bmod 1$. For the one-particle Green's function, they are given by $\triangle D=1/2$ and $\triangle N=1$. Thus the critical exponent η_F is defined as

$$\eta_F:=2\triangle=\frac{1}{2}\left(Z(\mathcal{K}_F)^2+\frac{1}{Z(\mathcal{K}_F)^2}\right). \tag{B4}$$

The dressed charge $Z(\mathcal{K}_F)$ is explicitly evaluated for two special cases[39]:

$$Z(\mathcal{K}_F)=\begin{cases}1 & \text{for } n_e=0 \ \ (\mathcal{K}_F=0)\\ \sqrt{\alpha/2} & \text{for } n_e=0.5 \ \ (\mathcal{K}_F=\infty),\end{cases} \tag{B5}$$

where α is

$$\alpha=\frac{\pi}{\pi-2\eta}. \tag{B6}$$

Then the critical exponent η_F is given by

$$\eta_F=\begin{cases}1 & \text{for } n_e=0\\ 1/\alpha+\alpha/4 & \text{for } n_e=0.5.\end{cases} \tag{B7}$$

In the scaling limit where CFT is valid, the correlation functions at $T\ll 1$ are recovered by the replacement

$$x\to\frac{v_F}{\pi T}\sinh\frac{\pi T x}{v_F}. \tag{B8}$$

in the denominator in Eq. (B1). Here v_F denotes the Fermi velocity

$$v_F:=\frac{1}{2\pi\rho(x)}\left.\frac{\partial\varepsilon(x)}{\partial x}\right|_{x=\mathcal{K}_F}. \tag{B9}$$

Note that $\rho(x)$ and $\varepsilon(x)$ are the density function and the dressed energy defined by

$$\rho(x)+\frac{1}{2\pi}\int_{-\mathcal{K}_F}^{\mathcal{K}_F}R(x-y)\rho(y)dy=\frac{\sin 2\eta}{\pi(\cosh 2x-\cos 2\eta)},\tag{B10}$$

$$\varepsilon(x)+\frac{1}{2\pi}\int_{-\mathcal{K}_F}^{\mathcal{K}_F}R(x-y)\varepsilon(y)dy=-\frac{\sin^2 2\eta}{\cosh 2x-\cos 2\eta}+\mu.$$

Thus the long-distance behavior of one-particle Green's function is given by

$$\langle c^{\dagger}(x)c(0)\rangle \sim \cos(k_F x)x^{-\pi\eta_F|x|T/v_F}.\tag{B11}$$

Consequently the correlation length at $T\ll 1$ is identified with

$$\xi=\frac{v_F}{\pi\eta_F T}.\tag{B12}$$

The Fermi velocity (B9) is analytically calculated for the cases $n_e\ll 1$ and $n_e=0.5$:

$$v_F=\begin{cases}\sim \pi n_e & \text{for } n_e\ll 1\\ \pi\sin 2\eta/4\eta & \text{for } n_e=0.5.\end{cases}\tag{B13}$$

Therefore, we obtain the explicit correlation length (B12) for these two special cases.

$$\xi T=\begin{cases}\sim n_e & \text{for } n_e\ll 1\\ \sin 2\eta/[4\eta(1/\alpha+\alpha/4)] & \text{for } n_e=0.5.\end{cases}\tag{B14}$$

We have also verified the extrapolations from the NLIE's agree with prediction (B12).

Finally we remark on the spin correlation. The main contribution to the transverse correlation function simply decays algebraically,

$$\langle \sigma^{+}(x)\sigma^{-}(0)\rangle \sim 1/x^{2\triangle'},\tag{B15}$$

that has no oscillation term. Here $\triangle'$ takes the *identical* form (B2). However, we have to use $\triangle N=1$ and $\triangle D=0$ this time. The difference in selection rules for these integers, which originates from the difference in statistics, leads to a conclusion

$$\triangle\neq\triangle'=\frac{1}{4Z(\mathcal{K}_F)^2}\tag{B16}$$

The corresponding correlation length is given by Eq. (B12), replacing η_F by $\eta_S=\frac{1}{2}[Z(\mathcal{K}_F)]^2$. One thus obtains different correlation lengths simply according to the selection rules.

APPENDIX C: DERIVATION OF NLIE's

For simplicity in notation we define

$$\mathfrak{c}(x):=\mathfrak{a}(x+i\gamma_1),\quad \mathfrak{C}(x):=1+\mathfrak{c}(x),$$
$$\bar{\mathfrak{c}}(x):=\mathfrak{a}(x-i\gamma_2),\quad \bar{\mathfrak{C}}(x):=1+\bar{\mathfrak{c}}(x).\tag{C1}$$

That is, we forget additional shifts for a moment.

We identify the analytic strips

$$Q(x):\quad \mathrm{Im}\,x\in(-2p_0,0),$$
$$\phi_-(x):\quad \mathrm{Im}\,x\in[0,2p_0),\tag{C2}$$
$$\phi_+(x):\quad \mathrm{Im}\,x\in(-2p_0,0].$$

The following identities are direct consequence of the definitions:

$$\Lambda(x+i)=\mathfrak{C}(x)\frac{Q(x-i)}{Q(x-(2p_0-1)i)}\phi_-(x+i)\times\phi_+(x-i(2p_0-3))e^{-\beta\mu/2},$$
$$\Lambda(x-i)=(-1)^{N/2+N_e}\bar{\mathfrak{C}}(x)\frac{Q(x-(2p_0-1)i)}{Q(x-i)}\times\phi_+(x-i)\phi_-[x+i(2p_0-3)]e^{\beta\mu/2}.\tag{C3}$$

Now we consider the second largest eigenvalue case $N_e=N/2-1$. We are in a position to utilize the knowledge of zeros of $\Lambda_2(x)$.

Consider the integral

$$\int_{\mathcal{C}}\frac{d}{dz}\ln\Lambda_2(z)e^{ikz}dz,$$

where $\mathcal{C}$ encircles the edges of "square:" $[z_1,z_2]\cup[z_2,z_3]\cup[z_3,z_4]\cup[z_4,z_1]$ in a counterclockwise manner, where $z_1=-\infty-i$, $z_2=\infty-i$, $z_3=\infty+i$, and $z_4=-\infty+i$. There is one zero of $\Lambda_2(x)$ in the region inside $\mathcal{C}$. Thus Cauchy's theorem is applied after proper modification as in Eq. (D4):

$$2\pi i e^{ik\theta}=\int_{-\infty}^{\infty}\frac{d}{dx}\ln\Lambda_2(x-i)e^{ik(x-i)}dx-\int_{-\infty}^{\infty}\frac{d}{dx}\ln\Lambda_2(x+i)e^{ik(x+i)}dx.\tag{C4}$$

One substitutes Eq. (C3) into the above equation and derives identities among the Fourier components of logarithmic derivatives of Q, $\mathfrak{C}$, and $\bar{\mathfrak{C}}$. Explicitly, we have

$$\widehat{dl}Q[k]=-\frac{e^{k(p_0-1)}\widehat{dl}\mathfrak{C}[k]-e^{k(p_0+1)}\widehat{dl}\bar{\mathfrak{C}}[k]}{4\sinh(p_0-1)k\cosh k}+\frac{e^{k(2p_0-1)}\widehat{dl}\phi_-[k]+e^{k}\widehat{dl}\phi_+[k]}{2\cosh k}-\frac{\pi i e^{k(p_0+i\theta)}}{2\sinh(p_0-1)k\cosh k}.\tag{C5}$$

In the above we adopt a notation

$$\widehat{dl}\mathfrak{C}[k]:=\int_{-\infty}^{\infty}\frac{d\ln\mathfrak{C}(x)}{dx}e^{ikx}dx,\tag{C6}$$

etc., as the Fourier component of the logarithmic derivatives.

On the other hand, from definition (C1), we have

$$\widehat{dl}\mathfrak{c}[k]=2\widehat{dl}\phi_-[k]\ e^{kp_0}\sinh(p_0-1)k -2\widehat{dl}\phi_+[k]\ e^{-(2p_0-2)k}\sinh k -2\widehat{dl}Q[k]\ e^{-(p_0-1)k}\sinh(p_0-2)k, \quad \text{(C7)}$$

and similarly for $\widehat{dl}\bar{\mathfrak{c}}[k]$.

One substitutes Eq. (C5) into Eq. (C7) to obtain a closed equation among the Fourier modes of the auxiliary functions.

Using the explicit form for $\phi_\pm$, we obtain

$$\widehat{dl}\mathfrak{c}[k]=-2\pi i\frac{N}{2}\frac{\sinh u_N k}{\cosh k}+\widehat{dl}\mathfrak{C}\frac{\sinh(p_0-2)k}{2\cosh k\sinh(p_0-1)k} -\widehat{dl}\bar{\mathfrak{C}}\frac{e^{2k}\sinh(p_0-2)k}{2\cosh k\sinh(p_0-1)k} +2\pi i e^{k+ik\theta}\frac{\sinh(p_0-2)k}{2\cosh k\sinh(p_0-1)k}. \quad \text{(C8)}$$

By inverse transformation and integration over x we arrive at the NLIE's. Note that the integration constant is determined by the asymptotic values in Eqs. (3.2a) and (3.2b).

After introducing the shifts $\gamma_{1,2}$, one obtains the identical NLIE's in the main text, except for "driving terms," as we have not yet taken the Trotter limit $N\to\infty$. To be precise, the driving term for $\ln\mathfrak{a}(x)$ is

$$\frac{N}{2}\int_{-\infty}^{\infty}\frac{\sinh u_N k}{k\cosh k}e^{ik(x-i\gamma_1)}dk. \quad \text{(C9)}$$

Due to the combination of $u_N=-\beta\sin 2\eta/2\eta N$ and N entering above, the Trotter limit is carried out analytically. Then one ends up with Eq. (3.3).

The expression for the eigenvalue is derived in a similar way. One first notes the "inversion identity"

$$\tilde{\Lambda}_2(x+i)\tilde{\Lambda}_2(x-i)=-\psi(x)\mathfrak{C}(x)\bar{\mathfrak{C}}(x), \quad \text{(C10)}$$

where

$$\psi(x):=\frac{\phi_+(x-i)\phi_-(x+i)}{\phi_+(x+i)\phi_-(x-i)} \quad \text{(C11)}$$

and

$$\tilde{\Lambda}_2(x)=\frac{\Lambda_2(x)}{\tanh\frac{\pi}{4}(x-\theta)\phi_+(x+2i)\phi_-(x-2i)} \quad \text{(C12)}$$

is introduced to exclude the zeros of $\Lambda_2(x)$ and to compensate for the divergence of $\Lambda_2(x)$ at $x\to\pm\infty$.

Then the left-hand side is ANZC in a strip $\mathrm{Im}\,x\in[-1,1]$ and also the right-hand side is ANZC in a narrow strip including the real axis. One thus can solve Eq. (C10), and obtain the expression

$$\ln\Lambda_2(x)=\ln\Lambda_{\mathrm{gs}}(x)+\ln\Lambda_{\mathrm{fn}}(x), \quad \text{(C13)}$$

where

$$\ln\Lambda_{\mathrm{gs}}(x):=-\frac{N}{2}\int_{-\infty}^{\infty}\frac{\sinh ku_N\sinh(p_0-1)k}{k\cosh k\sinh p_0 k}e^{-ikx}dk +\ln\phi_+(x+2i)\phi_-(x-2i), \quad \text{(C14a)}$$

$$\ln\Lambda_{\mathrm{fn}}(x):=K*\ln\mathfrak{A}(x+i\gamma_1)+K*\ln\bar{\mathfrak{A}}(x-i\gamma_2) +\ln\tanh\frac{\pi}{4}(x-\theta)-\frac{\pi i}{2}. \quad \text{(C14b)}$$

Taking the Trotter limit $N\to\infty$ after setting $x=0$, and using the identity

$$\lim_{N\to\infty}\ln\phi_+(2i)\phi_-(-2i)=-\frac{\beta}{2}\Delta, \quad \text{(C15)}$$

we derive the first excited free energy as Eq. (3.6).

Next we consider the largest eigenvalue sector $N_{\mathrm{e}}=N/2$. In this case, the spinless fermion model shares the same equations with the XXZ model. Then the following NLIE's have been already derived in Ref. 15:

$$\ln\mathfrak{a}_0(x)=-\frac{\pi\beta\sin(2\eta)}{4\eta\cosh\frac{\pi}{2}(x-i\gamma_1)}+F*\ln\mathfrak{A}_0(x) -F*\ln\bar{\mathfrak{A}}_0(x+2i-i(\gamma_1+\gamma_2))+\frac{\beta\mu p_0}{2(p_0-1)}, \quad \text{(C16)}$$

$$\ln\bar{\mathfrak{a}}_0(x)=-\frac{\pi\beta\sin(2\eta)}{4\eta\cosh\frac{\pi}{2}(x+i\gamma_2)}+F*\ln\bar{\mathfrak{A}}_0(x) -F*\ln\mathfrak{A}_0(x-2i+i(\gamma_1+\gamma_2))-\frac{\beta\mu p_0}{2(p_0-1)},$$

where auxiliary functions $\mathfrak{a}_0$, etc., are defined in a similar way to Eq. (3.1). Note that their asymptotic values $|x|\to\infty$ are explicitly written as

$$\mathfrak{a}_0(x)=\exp(\beta\mu),\quad \bar{\mathfrak{a}}_0(x)=\exp(-\beta\mu). \quad \text{(C17)}$$

Through the above NLIE's, $\Lambda_1(x)$ is described as

$$\ln\Lambda_1(x)=\ln\Lambda_{\mathrm{gs}}(x)+K*\ln\mathfrak{A}_0(x+i\gamma_1)+K*\ln\bar{\mathfrak{A}}_0(x-i\gamma_2). \quad \text{(C18)}$$

Taking the Trotter limit $N\to\infty$, we obtain the free energy per site f as

$$f=-\frac{1}{\beta}\ln\Lambda_1(0)-\frac{1}{4}\Delta=\epsilon_0-\frac{1}{\beta}K*\ln\mathfrak{A}_0(i\gamma_1) -\frac{1}{\beta}K*\ln\bar{\mathfrak{A}}_0(-i\gamma_2), \quad \text{(C19)}$$

where ϵ_0 is the well-known ground-state energy per site,

$$\epsilon_0=-\int_{-\infty}^{\infty}K(x)\frac{\sin^2 2\eta}{\cosh 2\eta x-\cos 2\eta}+\frac{1}{4}\Delta. \quad \text{(C20)}$$

Though we do not analyze Eqs. (C16) and (C19) here, they are implicitly used in the evaluation of the correlation length.

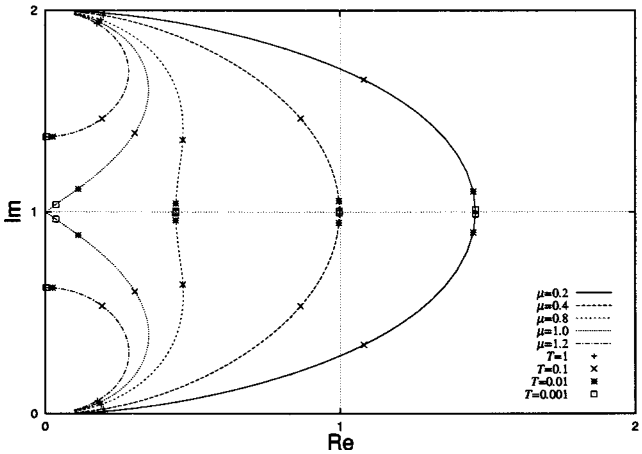

FIG. 10. The trajectories of the additional zeros for the free fermion model. The lower zero θ never goes over the physical strip, while the upper one θ' never comes into the strip. In the case $\mu=1.0$, both zeros moves to $\theta,\theta'=i$ at the low-temperature limit.

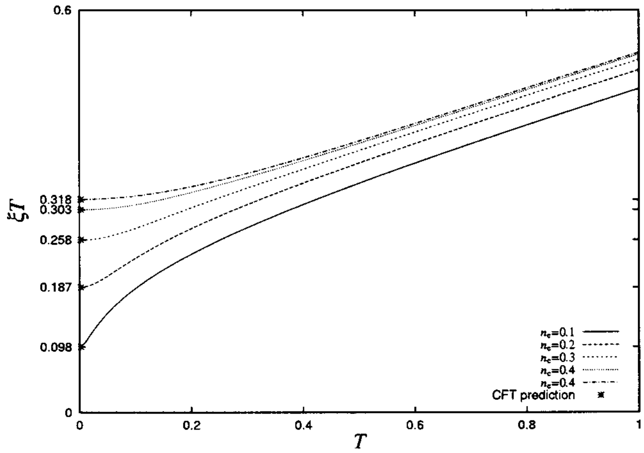

FIG. 11. The temperature dependence of the correlation length for the free fermion model.

APPENDIX D: FREE FERMION MODEL

Here we consider the free energy and the correlation length for the free fermion model $\Delta=0$ $(2\eta=\pi/2)$ in Eq. (2.1). In this case we have $\phi_{\pm}(x\pm 4i)=(-1)^{N/2}\phi_{\pm}(x)$ and $Q(x\pm 4i)=(-1)^{N_e}Q(x)$ from Eq. (2.53). Then Eq. (2.52) simplifies to

$$\Lambda(x)=\varrho(x)\frac{Q(x+2i)}{Q(x)}, \tag{D1}$$

where

$$\varrho(x):=\phi_-(x-2i)\phi_+(x)e^{(1/2)\beta\mu}+(-1)^{N/2}\phi_+(x+2i)\phi_-(x)e^{-(1/2)\beta\mu}. \tag{D2}$$

We can easily show that

$$\Lambda(x+i)\Lambda(x-i)=(-1)^{N_e}\varrho(x+i)\varrho(x-i). \tag{D3}$$

The right-hand side is a known function, which is a distinct feature of the free fermion model. It is convenient to modify the function $\Lambda(x)$ as

$$\tilde{\Lambda}(x)=\frac{\Lambda(x)}{\phi_+(x+2i)\phi_-(x-2i)}, \tag{D4}$$

satisfying

$$\tilde{\Lambda}(x+i)\tilde{\Lambda}(x-i)=(-1)^{(N/2)+N_e}[\psi(x)+\psi(x)^{-1}+2\cosh(\beta\mu)], \tag{D5}$$

where $\psi(x)$ was already defined in Eq. (C11).

First we consider the free energy characterized by the largest eigenvalue $\Lambda_1(x)$. It lies in the sector $N_e=N/2$. The Bethe ansatz root $\{x_j^{(1)}\}_{j=1}^{j=N/2}$, $\mathrm{Im}\,x_j^{(1)}\in[-1,1]$ are symmetric with respect to the imaginary axis. The function $\varrho(x)$ in Eq. (D2) has N zeros in $\mathrm{Im}\,x\in[-2,2]$: $N/2$ zeros $\{x_j\}_{j=1}^{N/2}$ are in the physical strip $\mathrm{Im}\,x\in[-1,1]$, and the others $\{x_j'\}_{j=1}^{N/2}$ are out of the strip. As $\varrho(x)$ has a property

$$\varrho(x+2i)|_{\mu}=(-1)^{N/2}\varrho(x)|_{-\mu}, \tag{D6}$$

we have

$$x_j'|_{\mu}=x_j|_{-\mu}+2i. \tag{D7}$$

From the BAE (2.54), $\{x_j^{(1)}\}$ are completely equivalent to $\{x_j\}$. Thereby one can shows from Eq. (D1) that $\Lambda_1(x)$ does not possess any zeros in the physical strip.

Since the function $\tilde{\Lambda}_1(x)$ is ANZC $\mathrm{Im}\,x\in[-1,1]$, we have

$$\ln\tilde{\Lambda}_1(x)=\{K*\ln[X+X^{-1}+2\cosh(\beta\mu)]\}(x). \tag{D8}$$

Using the relations

$$\lim_{N\to\infty}\psi(x)=\exp\left(\frac{\beta}{\cosh\frac{\pi x}{2}}\right),\qquad \lim_{N\to\infty}\tilde{\Lambda}(0)=\lim_{N\to\infty}\Lambda(0), \tag{D9}$$

we obtain the free energy per site f as

$$f=-\frac{1}{\beta}\lim_{N\to\infty}\ln[\Lambda_1(0)]=-\frac{1}{\pi\beta}\int_0^{\pi/2}\ln[2\cosh(\beta\cos\zeta)+2\cosh(\beta\mu)]d\zeta, \tag{D10}$$

in agreement with Ref. 43.

Next we consider the correlation length ξ for $\langle c_j^\dagger c_i\rangle$. The BAE roots $\{x_j^{(2)}\}_{j=1}^{N/2-1}$ relevant to the second largest eigenvalue are identical with $\{x_j^{(1)}\}_{j=1}^{N/2}$, except that the largest magnitude one $x_{N/2}^{(1)}=\theta$ is absent. Then $\Lambda_2(x)$ possesses the additional zero θ in the physical strip. In the Trotter limit, θ is given by

$$\theta=\frac{2}{\pi}\sinh^{-1}\left(\frac{\beta}{\pi-i\beta\mu}\right). \tag{D11}$$

The corresponding zero θ' through property (D7) is

$$\theta'=\frac{2}{\pi}\sinh^{-1}\left(\frac{\beta}{\pi+i\beta\mu}\right)+2i. \tag{D12}$$

The zero θ (θ') never goes over (never comes into) the physical strip (see Fig. 10).

Consequently, $\Lambda_2(x)$ can be expressed as

$$|\Lambda_2(x)| = \left|\Lambda_1(x)\tanh\frac{\pi}{4}(x-\theta)\right|. \tag{D13}$$

Thus we have the correlation length ξ for $\langle c_j^\dagger c_i \rangle$ as

$$\frac{1}{\xi} = -\ln\left|\tanh\left[\frac{1}{2}\sinh^{-1}\left(\frac{\beta}{\pi - i\beta\mu}\right)\right]\right| = \frac{1}{2}\left[\sinh^{-1}\left(\frac{\pi + i\beta\mu}{\beta}\right) + \sinh^{-1}\left(\frac{\pi - i\beta\mu}{\beta}\right)\right]. \tag{D14}$$

In Fig. 11 we plot the results [Eq. (D14)] for some fixed particle densities.

---

*Present address: Department of Physics, Faculty of Science, Shizuoka University, Ohya 836, Shizuoka, Japan.

[1] C. N. Yang and C. P. Yang, J. Math. Phys. **10**, 1115 (1969).
[2] M. Gaudin, Phys. Rev. Lett. **26**, 1301 (1971).
[3] M. Takahashi, Prog. Theor. Phys. **46**, 401 (1971).
[4] M. Takahashi and M. Suzuki, Prog. Theor. Phys. **48**, 2187 (1972).
[5] M. Suzuki, Phys. Rev. B **31**, 2957 (1985).
[6] M. Suzuki and M. Inoue, Prog. Theor. Phys. **78**, 787 (1987).
[7] M. Inoue and M. Suzuki, Prog. Theor. Phys. **79**, 645 (1988).
[8] T. Koma, Prog. Theor. Phys. **78**, 1213 (1987).
[9] J. Suzuki, Y. Akutsu, and M. Wadati, J. Phys. Soc. Jpn. **59**, 2667 (1990).
[10] J. Suzuki, T. Nagao, and M. Wadati, Int. J. Mod. Phys. B **6**, 1119 (1992).
[11] C. Destri and H. J. de Vega, Phys. Rev. Lett. **69**, 2313 (1992).
[12] M. Takahashi, Phys. Rev. B **43**, 5788 (1991).
[13] H. Mizuta, T. Nagao, and M. Wadati, J. Phys. Soc. Jpn. **63**, 3951 (1994).
[14] A. Klümper, Ann. Phys. (Leipzig) **1**, 540 (1992).
[15] A. Klümper, Z. Phys. B **91**, 507 (1993).
[16] G. Jüttner and A. Klümper, Europhys. Lett. **37**, 335 (1997).
[17] G. Jüttner, A. Klümper, and J. Suzuki, Nucl. Phys. B **487**, 650 (1997).
[18] G. Jüttner, A. Klümper, and J. Suzuki, J. Phys. A **30**, 1881 (1997).
[19] G. Jüttner, A. Klumper, and J. Suzuki, Nucl. Phys. B **512**, 581 (1998).
[20] G. Jüttner, A. Klümper, and J. Suzuki, Nucl. Phys. B **522**, 471 (1998).
[21] A. Kuniba, K. Sakai, and J. Suzuki, Nucl. Phys. B **525**, 597 (1998).
[22] A. Klümper, Eur. Phys. J. B **5**, 677 (1998).
[23] *Statistical Physics on the Eve of the 21st Century*, edited by M. T. Batchelor and L. T. Wille (World Scientific, Singapore, 1999).
[24] K. Fabricius, A. Klümper, and B. M. McCoy, cond-mat/9812012 (unpublished).
[25] J. Suzuki, Nucl. Phys. B **528**, 683 (1998).
[26] J. Suzuki, J. Phys. A **31**, 6887 (1998).
[27] J. Suzuki, J. Phys. A **32**, 2341 (1999).
[28] C. Scheeren, Ph.D. thesis, Universität zu Köln, 1998.
[29] F. C. Pu and B. H. Zhao, Phys. Lett. A **118**, 77 (1986).
[30] E. Olmedilla, M. Wadati, and Y. Akutsu, J. Phys. Soc. Jpn. **56**, 2298 (1987).
[31] E. Olmedilla and M. Wadati, J. Phys. Soc. Jpn. **56**, 4274 (1987).
[32] S. Murakami and F. Göhmann, Phys. Lett. A **227**, 216 (1997).
[33] F. Göhmann and S. Murakami, J. Phys. A **30**, 5269 (1997).
[34] M. Shiroishi, H. Ujino, and M. Wadati, J. Phys. A **31**, 2341 (1998).
[35] M. J. Martins and P. B. Ramos, Nucl. Phys. B **522**, 413 (1998).
[36] C. Destri and T. Segalini, Nucl. Phys. B **455**, 759 (1995).
[37] Y. Umeno, M. Shiroishi, and M. Wadati, J. Phys. Soc. Jpn. **67**, 1930 (1998).
[38] Y. Umeno, M. Shiroishi, and M. Wadati, J. Phys. Soc. Jpn. **67**, 2242 (1998).
[39] V. E. Korepin, N. M. Bogoliubov, and A. G. Izergin, *Quantum Inverse Scattering Method and Correlation Functions* (Cambridge University Press, Cambridge, 1993).
[40] A. Klümper and P. Pearce, J. Stat. Phys. **64**, 13 (1991).
[41] N. Kawakami and S.-K. Yang, *Conformal Field Theory and One-Dimensional Quantum Systems*, (Iwanami, Tokyo, 1997) (in Japanese).
[42] K. Sakai, J. Phys. Soc. Jpn. **68**, 1789 (1999).
[43] S. Katsura, Phys. Rev. **127**, 1508 (1962).